energies

Article

Heat and Mass Transfer in Structural Ceramic Blocks: An Analytical and Phenomenological Approach

Stephane K. B. M. Silva [1], Carlos J. Araújo [1], João M. P. Q. Delgado [2,*], Ricardo S. Gomez [1], Hortência L. F. Magalhães [3], Maria J. Figueredo [4], Juliana A. Figueirôa [5], Mirenia K. T. Brito [1], José N. O. Neto [6], Adriana B. C. Pereira [3], Leonardo P. L. Silva [7] and Antonio G. B. Lima [1]

1 Department of Mechanical Engineering, Federal University of Campina Grande, Campina Grande 58429-900, Brazil
2 CONSTRUCT-LFC, Department of Civil Engineering, Faculty of Engineering, University of Porto, 4200-465 Porto, Portugal
3 Department of Chemical Engineering, Federal University of Campina Grande, Campina Grande 58429-900, Brazil
4 Department of Agro-Industrial Management and Technology, Federal University of Paraíba, Bananeiras 58220-000, Brazil
5 Federal Institute of Education, Science and Technology of the Sertão Pernambucano, Petrolina 56316-686, Brazil
6 Integrated Colleges of Ceará, Iguatú 63508-025, Brazil
7 Department of Industry, Federal Institute Education, Science and Technology of Paraiba, Cajazeiras 58900-000, Brazil
* Correspondence: jdelgado@fe.up.pt; Tel.: +351-225081404

Citation: Silva, S.K.B.M.; Araújo, C.J.; Delgado, J.M.P.Q.; Gomez, R.S.; Magalhães, H.L.F.; Figueredo, M.J.; Figueirôa, J.A.; Brito, M.K.T.; Neto, J.N.O.; Pereira, A.B.C.; et al. Heat and Mass Transfer in Structural Ceramic Blocks: An Analytical and Phenomenological Approach. *Energies* **2022**, *15*, 7150. https://doi.org/10.3390/en15197150

Academic Editors: Kamel Hooman and Moghtada Mobedi

Received: 6 September 2022
Accepted: 21 September 2022
Published: 28 September 2022

Abstract: The ceramic industry is one of the pillars of the Brazilian economy, characterized by making low-cost products and an obsolete manufacturing process from a technological point of view. Among the various stages of production of ceramic materials, drying is one of the most energy-consuming and, in general, causes structural damage to the product, compromising its mechanical performance and final quality. Despite the relevance, studies on the drying of ceramic materials are mostly conducted at the experimental level and limited to some specific operational conditions. In this scenario, this research aims to theoretically study the heat and mass transfers in industrial ceramic blocks during drying. Based on the lumped analysis method, and considering the dimensional variations of the material, new phenomenological mathematical models and their respective analytical solutions are proposed to describe the kinetics of mass loss and heating of the material. The predicted results referring to the thermal and gravimetric behavior of the block during the oven drying process under different conditions are compared with the experimental data, obtaining excellent agreement between the results. Furthermore, the transport coefficients were estimated, proving the dependence of these parameters on the drying air conditions. The convective mass transfer coefficient ranged from 6.69×10^{-7} to 15.97×10^{-7} m/s on the outer surface of the block and from 0.70×10^{-7} to 1.03×10^{-7} m/s on the inner surface of the material when the drying air temperature ranged from 50 to 100 °C. The convective heat transfer coefficient ranged from 4.79 to 2.04 W/(m^2.°C) on the outer surface of the block and from 1.00 to 0.94 W/(m^2.°C) on the inner surface of the material when air temperature ranged from 50 to 100 °C.

Keywords: ceramic block; drying; lumped analysis; analytical; simulation

1. Introduction

Having been used for millennia, ceramics are characterized by their ability to conform when hydrated, which allows them to be molded for different uses, thus making them the main components for both artistic and industrial activities [1]. Considering its use in several activities, the ceramic sector is quite diversified, being divided into numerous segments and with emphasis on the red ceramic segment, which is linked to the civil construction industry, thus occupying a prominent place in the Brazilian economy [2,3] and worldwide.

The red ceramic segment is composed of numerous industries, characterized by different levels of technological development and production potential whose most representative elements are materials for civil construction (roof tiles, blocks, bricks, etc.). It is a sector that encompasses a series of different processes and raw materials, giving rise to several products which can be classified according to their physicochemical properties, chemical compositions, and applications [4–6].

Ceramic blocks are essential components for structural masonry, since they are responsible for providing mechanical strength, durability, and thermal comfort to buildings. These materials are characterized by having a low manufacturing cost, encompassing the stages of exploration of deposits, beneficiation, homogenization, conformation, drying, and firing [7–9].

As one of the steps in the manufacturing of ceramic materials that presents the most hydric and thermal problems, drying is defined as a thermodynamic phenomenon in which there is an exchange of energy either by conduction, convection, or radiation, as well as a change in the state of water, where it changes from the liquid state to the vapor state and is then dragged by the fluid that surrounds the material, phenomena that occur simultaneously. The purpose of this step is the hygroscopic removal of the moisture inside the product. However, when done incorrectly, it can cause structural damage to the part, thus promoting the loss of the product. Therefore, an in-deep understanding in the moisture and heat transfer mechanisms inside these materials becomes of paramount importance for the ceramic industry [10–13] and academy.

Despite its importance, studies on the drying of ceramic materials are conducted mostly at an experimental level with specific operating conditions, and there are few studies that involve phenomenological mathematical modeling and numerical simulation. The use of mathematical simulations associated with drying kinetics enables the optimization of the drying process, allowing it to be carried out economically and in a shorter time. In this way, the use of computer codes can promote greater control of the drying process, thus allowing optimization in production so that raw material losses and process costs are reduced, and the productivity of companies in the ceramic sector is increased. In this context, the following research can be cited: (1) at the industrial dryer level [14–16], (2) at the ceramic block level using CFD [17–19], and (3) at the ceramic block level using a lumped model [20–22]. In these works, details about the drying period, drying rate, moisture migration mechanisms, and many others interesting topics in drying process theory can be found. Furthermore, we can be cite the following works: Brown [23], Gualtieri et al. [24], Dogru et al. [25], Ndukwu et al. [26], Karagiannis et al. [27], and Pujari et al. [28].

Although the use of numerical simulations to describe phenomena such as the drying process of a material is of great value, there is a scarcity of mathematical models that describe the simultaneous heat and mass transfer in hollow solids with three-dimensional geometries, mainly for models that consider the external effects of heating and evaporation of the vapor produced on the surface of the solid, including dimensional variations in the material, a frequent phenomenon in this process. Furthermore, we can mention the high computational time spent in simulations with commercial CFD software. Thus, it is necessary to deepen the study with the use of more complete models that incorporate parameters which explain the internal and external phenomena intrinsic to the process, especially when applied to solids with complex geometries, and that provide results in a short computational time, which is of great importance for decision making in the industry.

Given the above, the present study aims to analytically describe the convective drying process of structural ceramic blocks based on lumped analysis. The use of mathematical models to describe the phenomena of energy and mass transfer in these blocks aims to control and optimize the drying process, preventing this process from being carried out incorrectly and thus affecting the performance and quality of the final part. The central idea is to reduce the cost of the process, achieved by controlling the drying time, increasing the quality of the final product, and minimizing the waste of raw materials, which directly contributes to the reduction in environmental impact.

As innovative aspects of this research, the following can be highlighted: (a) the use of more complete phenomenological models, which consider several simultaneous physical phenomena such as heat and mass convection, evaporation, and dimensional variations in the product throughout the process, (b) the reduced computational time to obtain the results, allowing the effects of several process variables to be analyzed in a short time, (c) the versatility of the proposed model being applied to different materials and product shapes, (d) the application of the study to a product with industrial dimensions, supplied by the Brazilian industry's ceramic sector, and (e) the theme of worldwide interest, which will certainly reach the interest of readers. The choice of the structural brick occurred due to its large application in different countries, including Brazil.

2. Methodology

2.1. The Geometry of the Ceramic Block and the Physical Problem

This investigation presents a numerical analysis of the convective drying process (heat and mass transfer) of structural ceramic blocks, as shown in Figure 1. The analysis was carried out from the mathematical modeling and computational simulation of the process where, to describe it, a lumped analysis method was used, considering the energy and mass balances for the ceramic block and drying air.

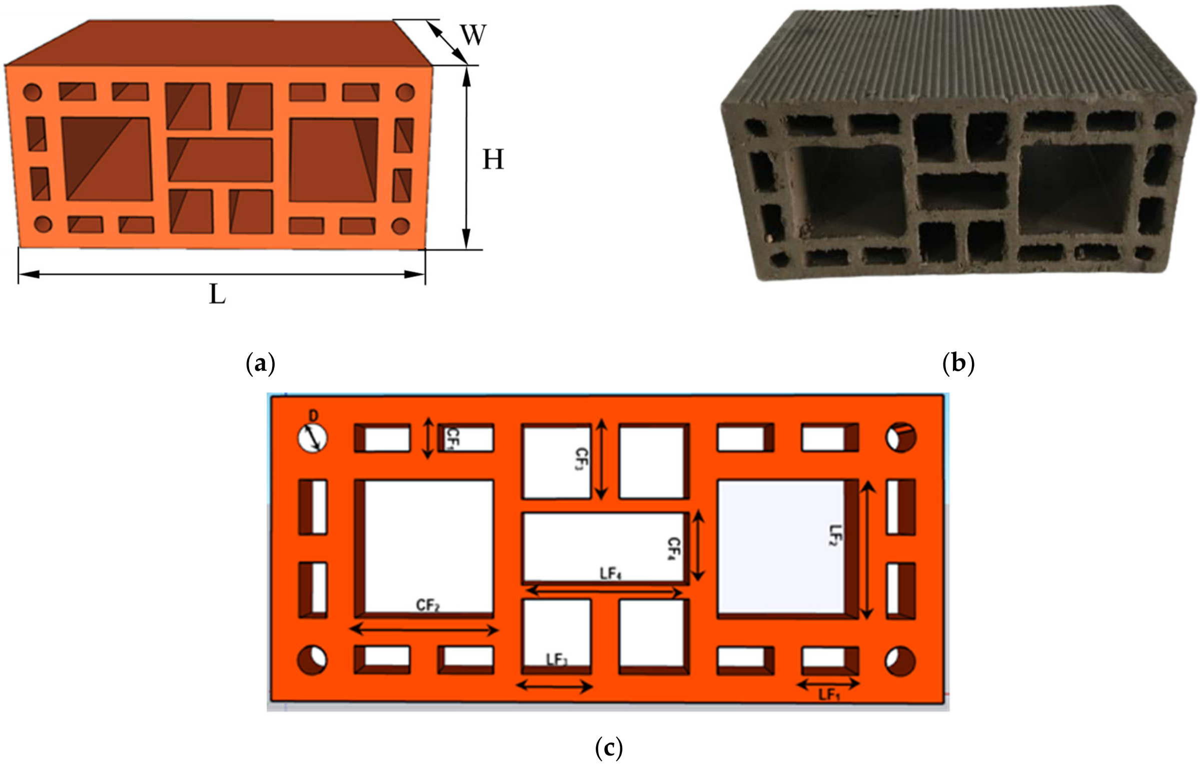

Figure 1. Structural ceramic block. (**a**) 3D drawing. (**b**) Photograph of the wet material. (**c**) Front view indicating the main dimensions of the material.

Table 1 summarizes the values of the characteristic dimensions of the ceramic block under study at the beginning of the drying process.

Table 1. Dimensions of the ceramic block before drying at different temperatures [14].

T (°C)	H (mm)	W (mm)	L (mm)	D (mm)	CF_1 (mm)	CF_2 (mm)	LF_1 (mm)	LF_2 (mm)	CF_3 (mm)	LF_3 (mm)	CF_4 (mm)	LF_4 (mm)
50	143	199	303	14	15	73	33	75	38	24	31	62
60	140	200	302	15	15	72	33	78	37	28	30	64
70	142	200	300	15	33	74	15	75	36	26	31	62
80	144	200	300	15	15	74	33	74	35	26	31	63
90	143	199	300	15	15	73	34	75	36	26	30	63
100	142	201	301	14	15	73	31	75	36	26	30	63

2.2. Mathematical Modeling

As is well known, the type of analysis chosen to describe a process limits the level of understanding that can be gained from this process [29]. In this research, the method of lumped analysis was chosen. In this method, the rates of heat and mass transfer between the product and air during the drying process neglect the intrinsic resistance of the product to these transfers.

Thus, to mathematically describe the process of energy and mass transfer in ceramic blocks, some hypotheses were considered: (a) The structural ceramic block is isotropic and consists of solid matter and water. (b) The mechanical and thermophysical properties of the material are constant throughout the process. (c) The water contained in the ceramic block, in its liquid state, migrates from the interior of the material, evaporating on its surface. (d) Drying occurs in the falling drying rate period (based on the experimental data of the moisture content throughout the process). (e) Drying occurs by the transport of heat and mass inside the solid, the convection of heat and mass, and evaporation at the surface. (f) Generations of energy and mass inside the material are negligible. Finally, (g) the drying process occurs with dimensional variation of the ceramic block.

2.2.1. Dimensional Analysis

In addition to the previously presented hypotheses, to numerically describe the process of heat and mass transfer in a ceramic block, as described in Figure 1, the dimensional variation models of the block during drying, proposed by Silva et al. [29], were used. The equations governing this model are as follows:

$$S_1(t) = S_{10}\left[a_1 + b_1 \times \mathrm{Exp}\left(-{k_1}^2 \times t\right)\right], \quad (1)$$

$$S_2(t) = S_{20}\left[a_2 + b_2 \times \mathrm{Exp}\left(-{k_2}^2\, t\right)\right], \quad (2)$$

$$V(t) = V_0\left[a_3 + b_3 \times \mathrm{Exp}\left(-{k_3}^2 \times t\right)\right], \quad (3)$$

where t is the time, V_0 and S_{i0} correspond to the volume and surface areas (external, i = 1 and internal, i = 2) at t = 0, respectively, and the variables a_1, b_1, k_1, a_2, b_2, k_2, a_3, b_3, and k_3 are parameters estimated from the non-linear adjustment to the experimental data in each drying condition. These parameters are described in Table 2.

Thus, based on the hypotheses established in the dimensional variation models, and considering the lumped analysis method, a phenomenological mathematical model was developed in order to describe the energy and mass transfers in the material. It is a complex but innovative model, since in the involved parameters, it considers the dimensional variations of the material during the drying process, as well as the phenomena of convective heat and mass transport and evaporation on the surface of the material. Details about the experimental procedure for measuring the dimensions of the brick along the drying process can be found in [14,20]. Details about the non-linear regression of Equations (1)–(3) to the experimental data are reported in [29]. However, we state that the determination coefficient ranged from 0.988 to 0.995, and the explained variance ranged from 97.6% to 99.1%.

Table 2. Statistical parameters of Equations (1–3), obtained after fitting to experimental data of the volume and surface area of the ceramic block throughout drying.

Parameter	T (°C)					
	50	60	70	80	90	100
a_1	0.901906	0.916317	0.913417	0.906832	0.918261	0.924380
b_1	0.094942	0.089238	0.090522	0.095390	0.081259	0.078334
k_1	−0.118153	−0.107296	−0.136887	−0.142611	−0.145465	−0.144425
a_2	0.934331	0.916679	0.936533	0.933251	0.930446	0.95068
b_2	0.078248	0.092013	0.076191	0.085057	0.077706	0.065325
k_2	−0.099675	−0.117138	−0.092472	−0.108381	−0.116544	−0.106260
a_3	0.827963	0.883788	0.845889	0.836882	0.868853	0.877361
b_3	0.156506	0.118260	0.168594	0.156642	0.127073	0.125252
k_3	−0.153099	−0.103415	−0.193381	−0.185467	−0.195847	−0.202705

2.2.2. Mass Transfer Model

Assuming a convective condition and performing a mass balance on the material, we can write

$$V\frac{d\overline{M}}{dt} = -h_{m1}S_1(\overline{M} - \overline{M}_e) - h_{m2}S_2(\overline{M} - \overline{M}_e) + \dot{M}V, \quad (4)$$

where V represents the volume of the block, h_{m1} and h_{m2} refer to the convective mass transfer coefficients on the outer and inner surfaces of the block, respectively, S_1 and S_2 represent the external and internal surface areas of the material, respectively, M and M_e are the moisture contents at time t and in the hygroscopic equilibrium condition, respectively, t is time, and $\dot{M}$ refers to mass generation inside the block.

Considering that there are no reactions that can generate moisture inside the block ($\dot{M} = 0$), and that $M = M_e$ at $t = 0$, when substituting in the mass balance model equations proposed by Silva et al. [29] for S_1, S_2, and V and solving the resulting ordinary differential equation, the following equation is obtained:

$$\frac{\overline{M} - \overline{M}_e}{\overline{M}_o - \overline{M}_e} = \mathrm{Exp}(A_M + B_M + C_M + D_M + E_M), \quad (5)$$

or

$$\overline{M} = (\overline{M}_o - \overline{M}_e)\mathrm{Exp}(A_M + B_M + C_M + D_M + E_M) + \overline{M}_e, \quad (6)$$

where

$A_M = \left(\frac{1}{a_{33}k_{11}k_{22}k_{33}}\right)\left[(-b_{11}k_{22}k_{33})\,{}_2F_1\left(1, \frac{k_{11}}{k_{33}}, \frac{k_{11}+k_{33}}{k_{33}}, -\frac{b_{33}}{a_{33}}\right)\right]$

$B_M = b_{11}\mathrm{Exp}(k_{11}t)k_{22}k_{33}\,{}_2F_1\left(1, \frac{k_{11}}{k_{33}}, \frac{k_{11}+k_{33}}{k_{33}}, -\frac{b_{33}\mathrm{Exp}(k_{33}t)}{a_{33}}\right)$

$C_M = k_{11}\left[-b_{22}k_{33}\,{}_2F_1\left(1, \frac{k_{22}}{k_{33}}, \frac{k_{22}+k_{33}}{k_{33}}, -\frac{b_{33}}{a_{33}}\right)\right]$

$D_M = b_{22}\mathrm{Exp}(k_{22}t)k_{33}\,{}_2F_1\left(1, \frac{k_{22}}{k_{33}}, \frac{k_{22}+k_{33}}{k_{33}}, -\frac{b_{33}\mathrm{Exp}(k_{33}t)}{a_{33}}\right)$

$E_M = (a_{11} + a_{22})k_{22}\{[k_{33}t + \ln(a_{33} + b_{33})] - \ln[a_{33} + b_{33}\mathrm{Exp}(k_{33}t)]\}$

where $a_{11} = h_{m_1}S_{10}a_1$, $b_{11} = h_{m_1}S_{10}b_1$, $k_{11} = -k_1{}^2$, $a_{22} = h_{m_2}S_{20}a_2$, $b_{22} = h_{m_2}S_{20}b_2$, $k_{22} = -k_2{}^2$, $a_{33} = V_0a_3$, $b_{33} = V_0b_3$, and $k_{33} = -k_3{}^2$. The term ${}_2F_1(a, b, c, z)$ is the ordinary hypergeometric function or hypergeometric Gauss series. For a better understanding, in the interval of $|z| < 1$, the hypergeometric function is defined by the following infinite series:

$$ {}_2F_1(a,b,c,z) = \sum_{n=0}^{\infty}\left[\frac{(a)_n \times (b)_n}{(c)_n} \times \frac{z^n}{n!}\right] = 1 + \frac{a \times b}{c} \times \frac{z}{1!} + \frac{a \times (a+1) \times b \times (b+1)}{c \times (c+1)} \times \frac{z^2}{2!} + \ldots, \quad (7) $$

where the term $(m)_n = m(m+1)(m+2)\ldots$ is the Pochhammer symbol. By definition, the value $(m)_0 = 1$ [30,31].

From Equation (6), it is possible to predict the behavior of mass transfer in a structural ceramic block by considering all the dimensional variations of the block during the drying process.

2.2.3. Heat Transfer Model

Analogous to the mass transfer, in the analysis of the heat transfer, it is assumed that the phenomena of thermal convection, evaporation, and heating of the produced vapor occur simultaneously on the surface of the block. In this way, the energy balance equation will be given by

$$ \rho_u V c_p \frac{d\overline{\theta}}{dt} = h_{c1}S_1(\overline{\theta}_\infty - \overline{\theta}) + h_{c2}S_2(\overline{\theta}_\infty - \overline{\theta}) + \rho_s V \frac{d\,\overline{M}}{dt}\left[h_{fg} + c_v(\overline{\theta}_\infty - \overline{\theta})\right] + \dot{q}\,V, \quad (8) $$

where ρ_u is the density of the wet ceramic block, c_p is the specific heat of the block, h_{c1} and h_{c2} correspond to the convective heat transfer coefficients (1 (external) and 2 (internal)), ρ_s refers to the density of the dry block, h_{fg} is the latent heat of vaporization of the free water, c_v is the specific heat of the water vapor, $\overline{\theta}_\infty$ and $\overline{\theta}$ are the temperatures of the external medium and the block at any time t of the process, respectively, and $\dot{q}$ corresponds to the internal heat generation. The term $\rho_s V \frac{d\,\overline{M}}{dt}$ represents the amount of water evaporated from the surface of the material per unit of time.

By neglecting the effects of mass transfer on heat transfer and internal energy generation (i.e., ($\frac{d\,\overline{M}}{dt} = 0$ and $\dot{q} = 0$)), substituting Equations (1–3) into Equation (8), considering the initial condition $\overline{\theta} = \overline{\theta}_o$ at t = 0, and performing the solution of the resulting ordinary differential equation, the following mathematical equation was obtained:

$$ \frac{\overline{\theta}_\infty - \overline{\theta}}{\overline{\theta}_\infty - \overline{\theta}_o} = \mathrm{Exp}(A_T + B_T + C_T + D_T + E_T), \quad (9) $$

or

$$ \overline{\theta} = (\overline{\theta}_\infty - \overline{\theta}_o)\mathrm{Exp}(A_T + B_T + C_T + D_T + E_T) + \overline{\theta}_\infty, \quad (10) $$

where

$$ A_T = \left(\frac{1}{\hat{a}_{33}\hat{k}_{11}\hat{k}_{22}\hat{k}_{33}}\right)\left[\left(-\hat{b}_{11}\hat{k}_{22}\hat{k}_{33}\right){}_2F_1\left(1, \frac{\hat{k}_{11}}{\hat{k}_{33}}, \frac{\hat{k}_{11}+\hat{k}_{33}}{\hat{k}_{33}}, -\frac{\hat{b}_{33}}{\hat{a}_{33}}\right)\right] $$

$$ B_T = \hat{b}_{11}\mathrm{Exp}(\hat{k}_{11}t)\hat{k}_{22}\hat{k}_{33}{}_2F_1\left(1, \frac{\hat{k}_{11}}{\hat{k}_{33}}, \frac{\hat{k}_{11}+\hat{k}_{33}}{\hat{k}_{33}}, -\frac{\hat{b}_{33}\mathrm{Exp}(\hat{k}_{33}t)}{\hat{a}_{33}}\right) $$

$$ C_T = \hat{k}_{11}\left[-\hat{b}_{22}\hat{k}_{33}{}_2F_1\left(1, \frac{\hat{k}_{22}}{\hat{k}_{33}}, \frac{\hat{k}_{22}+\hat{k}_{33}}{\hat{k}_{33}}, -\frac{\hat{b}_{33}}{\hat{a}_{33}}\right)\right] $$

$$ D_T = \hat{b}_{22}\mathrm{Exp}(\hat{k}_{22}t)\hat{k}_{33}{}_2F_1\left(1, \frac{\hat{k}_{22}}{\hat{k}_{33}}, \frac{\hat{k}_{22}+\hat{k}_{33}}{\hat{k}_{33}}, -\frac{\hat{b}_{33}\mathrm{Exp}(\hat{k}_{33}t)}{\hat{a}_{33}}\right) $$

$$ E_T = (\hat{a}_{11} + \hat{a}_{22})\hat{k}_{22}\{[\hat{k}_{33}t + \ln(\hat{a}_{33} + \hat{b}_{33})] - \ln[\hat{a}_{33} + \hat{b}_{33}\mathrm{Exp}(\hat{k}_{33}t)]\} $$

In Equation (10), the terms $\hat{a}_{11} = h_{c_1}S_{10}a_1$, $\hat{b}_{11} = h_{c_1}S_{10}b_1$, $\hat{k}_{11} = -k_1^2$, $\hat{a}_{22} = h_{c_2}S_{20}a_2$, $\hat{b}_{22} = h_{c_2}S_{20}b_2$, $\hat{k}_{22} = -k_2^2$, $\hat{a}_{33} = \rho_u C_p V_0 a_3$, $\hat{b}_{33} = \rho_u C_p V_0 b_3$, and $\hat{k}_{33} = -k_3^2$.

From Equation (10), it is possible to predict the behavior of heat transfer in a structural ceramic block while considering all the dimensional variation occurring in the block during the drying process.

2.3. Application to Structural Ceramic Blocks

In this research, emphasis is given to the drying of structural ceramic blocks. In order to determine the convective heat and mass transfer coefficients on the internal and external surfaces of the block, the results of the moisture content and temperature in the block, predicted by the proposed mathematical models, were compared with the experimental data of oven drying, as reported in [14,20].

According to Silva [14] and Silva et al. [20], in the beginning, during (at predetermined time intervals), and at the end of the drying process of the ceramic blocks, measurements of the dimensions, mass, and temperature (upper right vertex of the front face) of the ceramic block and the relative humidity, temperature, and velocity of the drying air inside the oven were made. Six (6) experimental tests were performed with different temperatures. At the end of each experiment, the dimensions, equilibrium mass, equilibrium temperature of the block, and total process time were obtained. Some data obtained by the authors can be found in Tables 3 and 4. These data were used in the computer simulation stage. Details about the data accuracy can be found in [14,20].

Table 3. Experimental parameters for the air and the ceramic block at the beginning of the drying process [14,20].

Test	Air			Ceramic Block			
	T (°C)	RH (%)	v (m/s)	M_0 (kg/kg, d.b.)	θ_o (°C)	ρ (kg/m^3)	c_p (J/kgK)
1	50	18.39	1.0	0.172319	31.5	1920	1673.51
2	60	12.27	1.0	0.173163	32.0	1920	1673.51
3	70	7.72	1.0	0.170186	29.8	1920	1673.51
4	80	4.99	1.0	0.172723	30.5	1920	1673.51
5	90	3.56	1.0	0.167900	27.6	1920	1673.51
6	100	2.34	1.0	0.169366	27.5	1920	1673.51

Table 4. Experimental parameters obtained after drying the ceramic block [14,20].

Test	M_e (kg/kg, d.b.)	θ_e (°C)	t (min)
1	0.002685	50.5	1170
2	0.001834	58.0	1050
3	0.001189	64.7	990
4	0.000826	68.6	930
5	0.000511	76.2	930
6	0.000054	95.1	750

To obtain the simulated results, the computer codes were developed in Mathematica® software. The comparison between the results predicted by the proposed mathematical model with the experimental data of the moisture content and temperature of the ceramic block was performed until a minimum error was reached. The squared deviations between the experimental and calculated values and the variance for the moisture content and temperature were obtained as follows:

$$\mathrm{MSE_M} = \sum_{i=1}^{n} \left(\overline{M}_{i,Num} - \overline{M}_{i,Exp}\right)^2, \tag{11}$$

$$\overline{S}^2_M = \frac{\mathrm{ERMQ_M}}{(n - \hat{n})}, \tag{12}$$

$$\mathrm{MSE}_{\theta} = \sum_{i=1}^{n} \left(\frac{\overline{\theta}_{i,\mathrm{Num}} - \overline{\theta}_{i,\mathrm{Exp}}}{\overline{\theta}_{\infty} - \overline{\theta}_{0}} \right)^{2}, \tag{13}$$

$$\overline{S}_{\theta}^{2} = \frac{\mathrm{ERMQ}_{\theta}}{(n - \hat{n})}, \tag{14}$$

where n is the number of experimental points and $\hat{n}$ is the number of fitted parameters (number of degrees of freedom) [32].

3. Results

3.1. Mass Transfer Analysis

As mentioned before, the estimation of the convective mass transfer coefficients on the external and internal surfaces of the ceramic block was made through a comparison between the moisture content data obtained by the proposed mathematical model and the data obtained experimentally by Silva [14] and Silva et al. [20]. The values obtained from these parameters as well as the mean squared error (MSE) are reported in Table 5.

Table 5. External (h_{m1}) and internal (h_{m2}) convective mass transfer coefficients for each drying temperature.

T (°C)	Convective Mass Transfer Coefficient		MSE$_M$ (kg/kg)^2
	hm$_1$ (m/s)	hm$_2$ (m/s)	
50	6.69×10^{-7}	0.70×10^{-7}	0.00174
60	8.80×10^{-7}	0.80×10^{-7}	0.00053
70	9.28×10^{-7}	1.00×10^{-7}	0.00030
80	11.84×10^{-7}	1.30×10^{-7}	0.00119
90	11.69×10^{-7}	1.03×10^{-7}	0.00027
100	15.97×10^{-7}	1.03×10^{-7}	0.00036

When evaluating the physical behavior of the convective mass transfer coefficient (Table 5), an increase in this parameter was observed with the increase in the drying temperature. It is well known that the increase in this thermo-physical parameter increases the drying rates of the ceramic block, causing hygroscopic equilibrium conditions to be reached more quickly. In addition, it is also possible to observe that the convective mass transfer coefficient obtained on the external surface of the ceramic block was greater than the coefficient of the internal surface of this block. This was due to the fact that the external surface area of the block in contact with the drying air was greater than the internal one, favoring the mass exchange between the product and the heated fluid surrounding the block. Additionally, it was noticed that the position of the block inside the oven contributed to the behavior of these parameters in each drying condition.

Regarding the values obtained for the mean squared error, low values of this statistical parameter can be observed, an indication of an excellent fit between the results predicted by the model and the experimental data and that the proposed mathematical model can adequately describe the drying process of ceramic blocks.

Confirming the data presented in Table 5, Figure 2 illustrates the predicted and experimental curves [14,20] of the moisture content of the ceramic block as a function of the drying time for different drying temperatures. When analyzing the behavior of the moisture content as a function of the processing time, it was possible to identify excellent agreement between the values predicted by the mathematical model and the experimental data, with a small deviation in the final process times mainly for low temperatures of drying. This can be attributed to the consideration of a constant mass transfer coefficient throughout the process being imposed on the model.

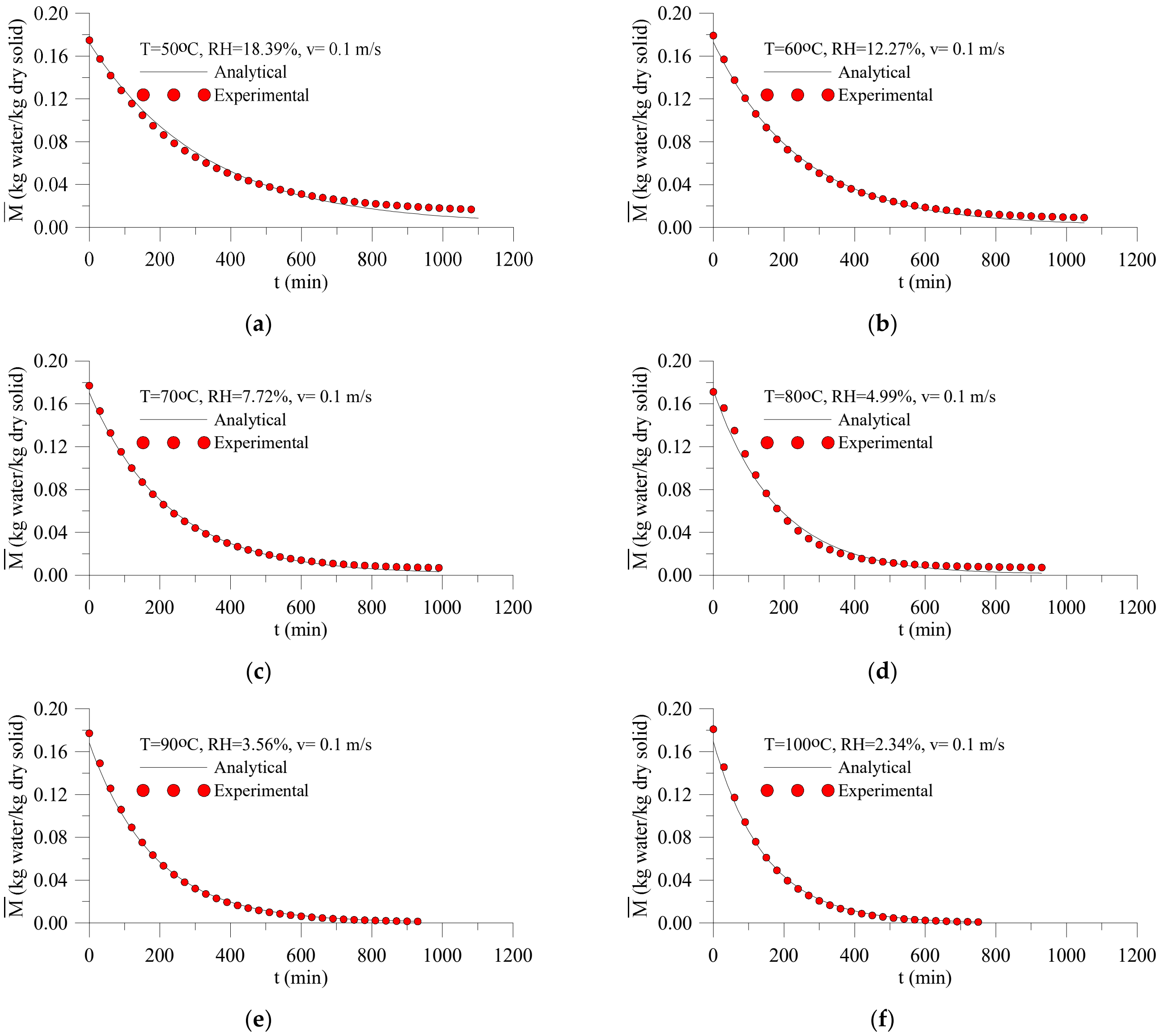

Figure 2. Transient behavior of predicted and experimental [14] moisture content of the ceramic block for different drying temperatures: (**a**) T = 50 °C, (**b**) T = 60 °C, (**c**) T = 70 °C, (**d**) T = 80 °C, (**e**) T = 90 °C, and (**f**) T = 100 °C.

When analyzing the moisture content curves from a physical point of view, there was a significant reduction in the moisture content in the first minutes of drying (high falling drying rate), as reported in [11,12,14,22].

For the lowest drying temperatures (from 50 °C to 70 °C), it was noted that more intense reduction in the moisture content occurred until the first 500 min (approximately 8.3 h) of the process. For higher temperatures (above 70 °C), this intense reduction occurred in a shorter process time, occurring up to the first 300 min (approximately 5 h). Thus, higher drying temperatures contributed to the material reaching its hygroscopic equilibrium in a shorter process time.

The variation in the moisture removal rate from the ceramic block was influenced by both the drying temperature and geometry of the material. It is well known that hollow ceramic blocks have better air circulation inside, which leads to a faster reduction in moisture. However, although its geometric shape provides a more accentuated reduction in the processing time, abrupt reductions in the moisture content can cause structural defects in the material, such as cracks and deformations, reducing the quality of the product at the end of drying. It is also important to highlight that in the first minutes of the drying stage, there is a large reduction in the dimensions of the solids (higher shrinkage speed), tending to remain constant after a long drying period, which can affect the quality of the product at the end of drying [13,15,17,18,21,24].

3.2. Heat Transfer Analysis

In a similar way to the procedure performed in the analysis of the mass transfer, the obtaining of the convective heat transfer coefficients on the external and internal surfaces of the ceramic block was given through a comparison between the predicted data and the experimental data [14,20] of the temperature at the vertex of the ceramic block until a smaller least square error was obtained. Table 6 summarizes the values of the convective heat transfer coefficients and the least square error for each drying temperature.

Table 6. Convective heat transfer coefficients for the external (h_{c1}) and internal (h_{c2}) areas for each drying temperature.

T (°C)	Convective Heat Transfer Coefficient		MSE_θ (-)
	hc_1 (W/m^2.°C)	hc_2 (W/m^2.°C)	
50	4.79	1.00	1.18412
60	2.19	1.06	4.08616
70	2.72	1.00	18.1275
80	2.41	0.37	4.99504
90	2.03	0.60	2.33426
100	2.04	0.94	1.12158

When analyzing Table 6, some observations can be made from the values obtained for the temperature and convective heat transfer coefficients. Differences between the predicted and experimental data of the vertex temperature can be attributed to the possible temperature measurement errors which occurred during the collection of experimental data, the fact that the model considered that the temperature of the material was the same throughout its volume at each time, and the neglected effects of the mass transfer on the heat transfer. It was observed that the convective coefficients obtained for the external surface of the ceramic block were higher than the convective coefficients obtained for the internal surface, proving that the block heated up more slowly inside. This is because the external surface of the block is more directly exposed to the drying air, allowing the convective heat flux to act with greater intensity in this region. However, even though the values obtained for the convective coefficients were low, typical of natural convection, it is noted that these coefficients did not assume an increasing behavior with the increase in the drying temperature. The divergence in the behavior of these thermo-physical parameters can be associated with possible temperature measurement errors which occurred during the collection of experimental data and the fact that the model considers that the temperature of the material is the same throughout its volume at each time, which clearly does not occur in practice, particularly for drying at high temperatures and a low relative humidity. Other factors can be listed: drying time, air relative humidity, shrinkage, and the different dimensions and moisture contents of the ceramic block at the beginning of drying.

It is known that higher values of the convective heat transfer coefficients provoke an increase in the heating rates, causing the material to reach the thermal equilibrium condition more quickly. On the other hand, high heating rates cause high temperature variation rates inside the material and, with this, high drying rates and thermal and hydric stresses, which in turn can cause severe drying problems such as cracks, warping, deformations, and ruptures, which considerably reduce the quality of the product in the firing stage [13,15,17,18,21].

Complementing the heat transfer analysis, Figure 3 illustrates the heating curves of the ceramic block for different drying temperatures (from 50 °C to 100 °C).

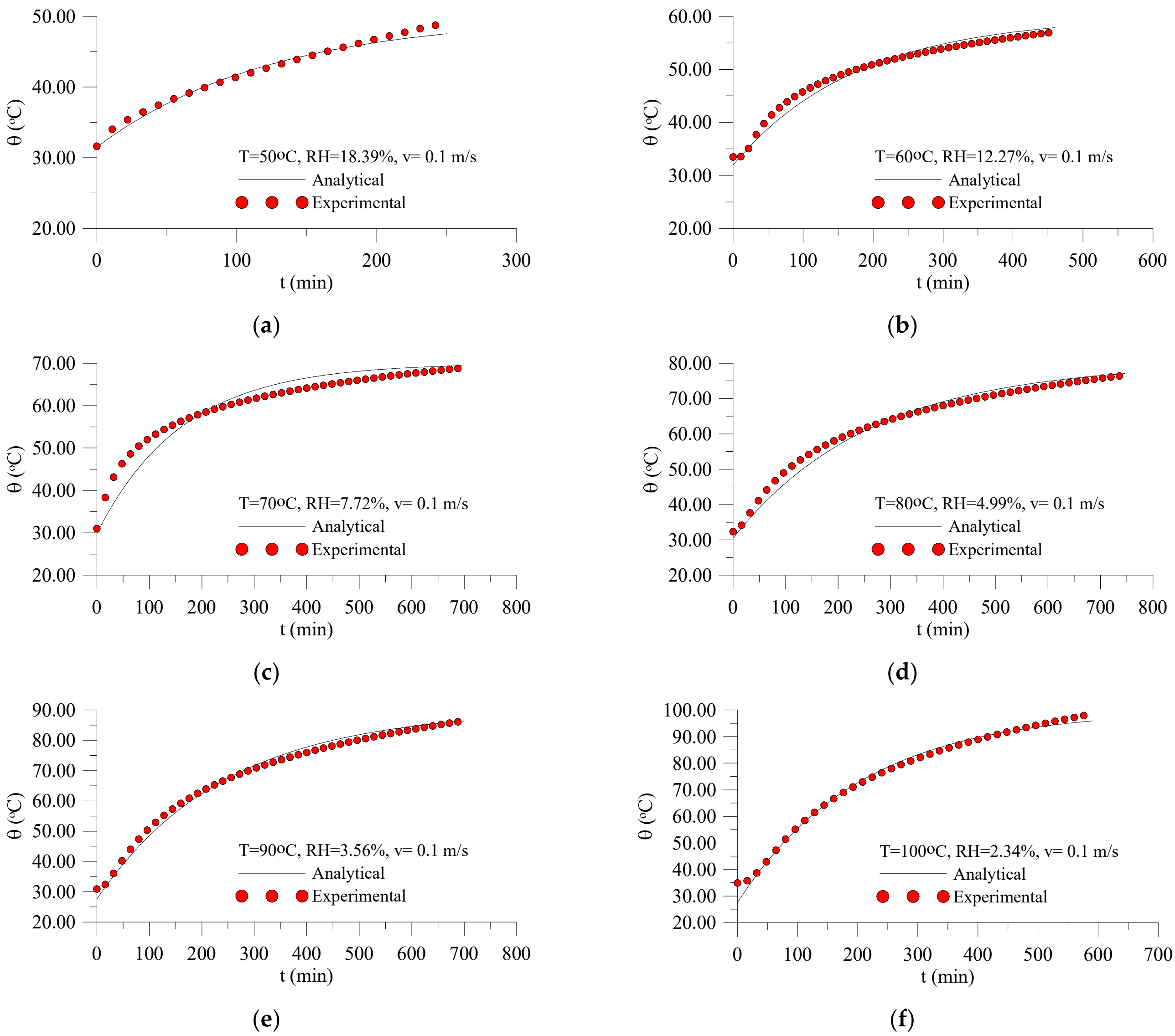

Figure 3. Transient behavior of experimental [14] and predicted temperatures of the ceramic block for different temperatures: (**a**) T = 50 °C, (**b**) T = 60 °C, (**c**) T = 70 °C, (**d**) T = 80 °C, (**e**) T = 90 °C, and (**f**) T = 100 °C.

Although the heat transfer coefficients showed a different behavior than expected, when analyzing the heating curves, a concordance between the values predicted by the model and the experimental data was observed, confirming once again that the proposed modeling was efficient for describing the drying process.

When analyzing the graphs, it was observed that the heating curves presented a behavior similar to that presented by the moisture content curves (Figure 2) since, for the lower drying air temperatures, a significant increase occurred for the temperature of the block until the first 300 min (5 h) of the process, and it then assumed an almost constant behavior once the block had almost completely reached its thermal equilibrium.

Although high drying temperatures imply a shorter process time, it is necessary to have strict control regarding this drying condition. As mentioned earlier, performing convective drying with high heating rates in an atmosphere with low relative humidity can lead to greater removal of the existing moisture in the solid, causing damage to the ceramic product and thus affecting its mechanical performance and quality when in operation.

In general, a comparison between the transport coefficients reported in the literature is very difficult due to the different parameter estimation methods used, the variation in the chemical composition of the ceramic material, and its physical and chemical structures.

The precision and accuracy of the measurements are important factors to consider when a method is good enough to be used in the estimation of some process parameters. In general, systematic errors around 5% and standard errors around 3% are expected due to, for example, limited instrument precision. Therefore, these errors are directly passed on to the estimation of transport coefficients. Other errors can be attributed to the different nature of the materials and the uncertainty in the experimental measurement, methodology, and geometric consideration of the body.

Despite this, the convective heat and mass transfer coefficients obtained in this study, compared with those reported in the literature and which are listed in Table 7, corroborated the effectiveness of the methodology used.

Table 7. Heat and mass transfer coefficients obtained in the drying of ceramic bricks reported in the literature.

Geometry	T (°C)	RH (%)	Convective Mass Transfer Coefficient (m/s)		Convective Heat Transfer Coefficient (W/m^2.°C)		Source
			hm_1	hm_2	hc_1	hc_1	
	50	20.8	2.87×10^{-7}		0.50		Silva et al. [22]
		20	1.67×10^{-7}	1.59×10^{-7}	5.34	5.11	Lima et al. [13]
	60	13.5	2.92×10^{-7}		0.58		Silva et al. [22]
		20	2.05×10^{-7}	1.96×10^{-7}	5.51	5.26	Lima et al. [13]
	70	7.6	4.95×10^{-7}		0.98		Silva et al. [22]
		20	2.46×10^{-7}	2.35×10^{-7}	5.64	5.39	Lima et al. [13]
	80	4.6	6.01×10^{-7}		0.96		Silva et al. [22]
		20	2.91×10^{-7}	2.78×10^{-7}	5.75	5.49	Lima et al. [13]
	90	3.3	6.03×10^{-7}		1.07		Silva et al. [22]
		20	3.43×10^{-7}	3.28×10^{-7}	5.84	5.58	Lima et al. [13]
	100	1.8	8.17×10^{-7}		1.74		Silva et al. [22]
		20	4.10×10^{-7}	3.92×10^{-7}	5.91	5.66	Lima et al. [13]
		1.8	6.47×10^{-7}	6.13×10^{-7}	6.89	6.54	Lima et al. [21]

Silva et al. [22]: lumped model considering a single heat and mass transfer coefficient estimated by non-linear regression and without dimensional variations. Lima et al. [13] and Lima et al. [21]: lumped model considering the existence of two heat and mass transfer coefficients determined by a proposed formulation and without dimensional variations.

In all the cases listed in Table 7, lumped models were used. Thus, the highest differences in the convective heat and mass transfer coefficient could mainly be attributed to the following factors:

(a) The type of lumped model;
(b) Considerations of the dimensional variations adopted in the model;
(c) The chemical composition of the product;
(d) The product's geometry;
(e) The equilibrium moisture content (hysteresis phenomenon in the sorption isotherm);
(f) The drying conditions (relative humidity and air velocity);
(g) Variations in the physical structure of the product (porosity, tortuosity, and permeability);
(h) The probable formation of pores by evaporation of water.

The convective heat transfer coefficient is not really a property of a material. It is used to quantify the rate of heat transfer at the surface of the body. It is dependent on the fluid velocity, fluid properties, surface roughness, and body shape, as well as the temperature difference between the surface and the fluid surrounding the body. In practice, the heat flux and surface temperature are very difficult to measure without disturbing the heat transfer and the flow of the heated fluid in the thermal and hydrodynamic boundary layers. In some materials with high moisture contents, heat transfer is accompanied by mass transfer, further complicating the measurement of the convective heat transfer coefficient.

Finally, as already mentioned, the convective heat and mass transfer coefficients are dependent on the velocity of the free air stream, but this effect is not explicitly stated in the model since the air velocity, in all experiments, remained practically constant (natural convection inside the oven). However, the low results of these parameters reflect this experimental condition, mainly inside the holes, where the air is confined, in contrast to what occurs on the external surface, where the air can flow by buoyant forces with no boundaries to impede its movement, which resulted in higher results for this parameter.

4. Conclusions

This study presents a numerical analysis of the drying process of structural ceramic blocks, where through phenomenological mathematical models based on lumped analysis, it was possible to analyze the transient heat and mass transfers that occurred in the ceramic block during the process. Thus, based on the analysis of the obtained results, it was verified that the phenomenological mathematical modeling used was effective for describing the heat and mass transfers of the ceramic block during the drying process. The effectiveness of the proposed models for predicting the heat and mass transfer phenomena, including dimensional variations of the ceramic block, was proven when it was observed that the discrepancies between the predicted and experimental results (reported in the literature) of the moisture content and temperature at the vertex of the ceramic block were small. Thus, it easily becomes possible to estimate the drying times of ceramic products with different shapes in different drying conditions in order to assist academy and industry in the decision making related to this complex physical problem.

From the results obtained, it was possible to estimate the convective mass transfer coefficients involved in the process. It was found that the convective mass transfer coefficient ranged from 6.69×10^{-7} to 15.97×10^{-7} m/s on the outer surface of the block and from 0.70×10^{-7} to 1.03×10^{-7} m/s on the inner surface of the material when the drying air temperature ranged from 50 to 100 °C. The convective heat transfer coefficient ranged from 4.79 to 2.04 W/(m^2.°C) on the outer surface of the block and from 1.00 to 0.94 W/(m^2.°C) on the inner surface of the material while the temperature of the drying air ranged from 50 to 100 °C. The low values for the convective heat and mass transfer coefficients are a strong indication that the mass removal and heating processes at the block surface occurred by natural convection.

Author Contributions: Conceptualization, S.K.B.M.S. and J.A.F.; methodology, S.K.B.M.S. and M.K.T.B.; software, S.K.B.M.S., J.N.O.N. and L.P.L.S.; validation, S.K.B.M.S. and M.J.F.; formal analysis, S.K.B.M.S.; investigation, S.K.B.M.S.; writing—original draft preparation, S.K.B.M.S. and H.L.F.M.; writing—review and editing, R.S.G. and J.M.P.Q.D.; visualization, A.B.C.P.; supervision, C.J.A. and A.G.B.L. All authors have read and agreed to the published version of the manuscript.

Funding: This research was funded by CAPES, CNPq, and FAPESQ-PB (Brazilian research agencies). In addition, this work was financially supported by base funding (UIDB/04708/2020) and programmatic funding (UIDP/04708/2020) of the Instituto de I&D em Estruturas e Construções (CONSTRUCT), funded by national funds through the FCT/MCTES (PIDDAC), and by the Fundação para a Ciência e a Tecnologia (FCT) through the individual Scientific Employment Stimulus 2020.00828.CEECIND.

Data Availability Statement: The data that support the findings of this study are available upon request from the authors.

Acknowledgments: The authors are grateful to CNPq, CAPES, FINEP, and FAPESQ-PB for the financial support and the researchers mentioned in the manuscript who, with their research, helped in the development of this work.

Conflicts of Interest: The authors declare no conflict of interest.

Nomenclature

c_p	Specific heat of the block	(J/kgK)
c_v	Specific heat of the water vapor	(J/kgK)
h_{c1}	Convective heat transfer coefficients (1, external)	(W/m^2K)
h_{c2}	Convective heat transfer coefficients (2, internal)	(W/m^2K)
h_{fg}	Latent heat of vaporization of free water	(J/kgK)
h_{m1}	Convective mass transfer coefficients (1, external)	(m/s)
h_{m2}	Convective mass transfer coefficients (2, internal)	(m/s)
H	Height	(mm)
L	Length	(mm)
M	Moisture content	(kg/kg, d.b.)
$\dot{M}$	Mass generation inside the block	($kg/kg/s/m^3$)
M_e	Hygroscopic equilibrium condition	(kg/kg, d.b.)
M_0	Initial moisture content	(kg/kg, d.b.)
MSE_M	Squared deviations for the moisture content	(-)
MSE_θ	Squared deviations for the temperature	(-)
n	Number of experimental points	(-)
$\hat{n}$	Number of fitted parameters	(-)
$\dot{q}$	Internal heat generation	(W/m^3)
RH	Air relative humidity	(%)
ρ	Density of the wet block	(kg/m^3)
ρ_s	Density of the dry block	(kg/m^3)
ρ_u	Density of the wet ceramic block	(kg/m^3)
S	Total surface area of the material	(m^2)
S_1	External surface area of the material	(m^2)
S_2	Internal surface area of the material	(m^2)
S_{i0}	Surface areas (external, i = 1 and internal, i = 2) at t = 0	(m^2)
$\overline{S}_M^2$	Variance for the moisture content	(-)
$\overline{S}_\theta^2$	Variance for the temperature	(-)
$\overline{\theta}$	Temperatures at any time t of the process	(°C)
$\overline{\theta}_\infty$	Temperatures of the external medium	(°C)
θ_e	Thermal equilibrium temperature	(°C)
θ_o	Initial temperature	(°C)
t	Time	(min)
T	Air temperature	(°C)
v	Air velocuty	(m/s)
V	Volume	(m^3)
V_0	Initial volume	(m^3)
W	Width	(mm)

References

1. Cavalcanti, M.S.L. Development of Ceramic Masses for Sanitary Stoneware Using Flat Glass Residue as a Flux in Partial Replacement of Feldspar. Ph.D. Thesis, Process Engineering, Federal University of Campina Grande, Campina Grande, Brazil, 2010. Available online: http://dspace.sti.ufcg.edu.br:8080/jspui/handle/riufcg/1778 (accessed on 10 November 2021). (In Portuguese)
2. Motta, J.F.M.; Zanardo, A.; Cabral, M., Jr. Ceramic raw materials. Part I: The profile of the main ceramic industries and their products. *Cerâm. Ind.* **2021**, *6*, 28–39. Available online: https://ceramicaindustrial.org.br/article/5876570b7f8c9d6e028b4643/pdf/ci-6-2-5876570b7f8c9d6e028b4643.pdf (accessed on 6 June 2022). (In Portuguese)
3. Bellingieri, J.C. The origins of the ceramic industry in São Paulo. *Cerâm. Ind.* **2005**, *10*, 19–23. Available online: http://host-article-assets.s3.amazonaws.com/ci/587657237f8c9d6e028b46d1/fulltext.pdf (accessed on 7 June 2022). (In Portuguese)

4. Almeida, G.S. Simulation and Experimentation of the Drying of Red Ceramics in Industrial Thermal Systems. Ph.D. Thesis, Process Engineering, Federal University of Campina Grande, Campina Grande, Brazil, 2009. Available online: http://dspace.sti.ufcg.edu.br:8080/xmlui/handle/riufcg/11369 (accessed on 12 November 2021). (In Portuguese)
5. Prado, U.S.; Bressiani, J.C. Overview of the Brazilian ceramic industry in the last decade. *Cerâm. Ind.* **2013**, *18*, 7–11. Available online: http://repositorio.ipen.br/bitstream/handle/123456789/17430/18423.pdf?sequence=1 (accessed on 7 June 2022). (In Portuguese) [CrossRef]
6. Cabral, M., Jr.; Azevedo, P.B.M.; Cuchierato, G.; Motta, J.F.M. Strategic study of the ceramic industry production chain in the state of São Paulo: Part I—Introduction and the red ceramic industry. *Cerâm. Ind.* **2019**, *24*, 20–34. [CrossRef]
7. Martinez, P.H. Influence of Ceramic Block Geometry on the Behavior of Structural Masonry Wall Beams. Master's Thesis, Civil Engineering, Paulista State University, Ilha Solteira, Brazil, 2017. Available online: https://repositorio.unesp.br/handle/11449/148961 (accessed on 15 November 2021). (In Portuguese)
8. Santos, R.S. Study of the Drying Process of Structural Ceramic Blocks: Modeling and Simulation. Ph.D. Thesis, Process Engineering, Federal University of Campina Grande, Campina Grande, Brazil, 2019. Available online: http://dspace.sti.ufcg.edu.br:8080/xmlui/handle/riufcg/10549 (accessed on 18 November 2021). (In Portuguese)
9. Santos, I.A.P. *Structural Masonry and a Comparative Analysis between Ceramic and Concrete Blocks*; Course Final Report (Undergraduate Course in Civil Engineering); Federal University of Campina Grande: Pombal, Brazil, 2021; Available online: http://dspace.sti.ufcg.edu.br:8080/xmlui/handle/riufcg/21732 (accessed on 21 November 2021). (In Portuguese)
10. Ibrahim, M.H.; Daud, W.R.W.; Talib, M.Z.M. Drying Characteristics of Oil Palm Kernels. *Dry. Technol.* **1997**, *15*, 1103–1117. [CrossRef]
11. de Brito, M.T.; de Almeida, D.T.; de Lima, A.B.; Rocha, L.A.; de Lima, E.S.; de Oliveira, V.B. Heat and Mass Transfer during Drying of Clay Ceramic Materials: A Three-Dimensional Analytical Study. *Diffus. Found.* **2017**, *10*, 93–106. [CrossRef]
12. Nascimento, J.J.D.S.; Luna, C.B.B.; Costa, R.F.; Barbieri, L.F.P.; Bezerra, E.D.O.T. Evaluation of red clay and ball clay drying using transient three-dimensional mathematical modeling: Volumetric shrinkage and moisture content. *Mater. Res. Express* **2019**, *6*, 95206. [CrossRef]
13. Lima, E.S.; Lima, W.M.P.B.; Silva, S.K.B.M.; Magalhães, H.L.F.; Nascimento, L.P.C.; Gomez, R.S.; Lima, A.G.B. Drying of industrial ceramic bricks and process parameter estimation: An advanced concentrated approach. *Res. Soc. Dev.* **2020**, *9*, e48391211391. [CrossRef]
14. Silva, A.M.V. Drying of Industrial Ceramic Blocks: Modeling, Simulation and Experimentation. Ph.D. Thsis, Process Engineering, Federal University of Campina Grande, Campina Grande, Brazil, 2018. Available online: http://dspace.sti.ufcg.edu.br:8080/jspui/handle/riufcg/7173 (accessed on 23 November 2021). (In Portuguese)
15. Tavares, F.V.D.S.; Cavalcante, A.M.D.M.; de Figueiredo, M.J.; Vilela, A.F.; de Lima, A.R.C.; Azerêdo, L.P.M.; de Lima, A.G.B. On the Modeling of Drying Process in an Industrial Tunnel Dryer. *Defect Diffus. Forum* **2020**, *400*, 51–56. [CrossRef]
16. Gomez, R.S.; Porto, T.R.N.; Magalhães, H.L.F.; Guedes, C.A.L.; Lima, E.S.; Wanderley, D.M.A.; Lima, A.G.B. Transient Thermal Analysis in an Intermittent Ceramic Kiln with Thermal Insulation: A Theoretical Approach. *Adv. Mater. Sci. Eng.* **2020**, *2020*, 6476723. [CrossRef]
17. Santos, R.S.; de Farias Neto, S.R.; de Lima, A.G.B.; Silva Júnior, J.B.; da Silva, A.M.V. Drying of Ceramic Bricks: Thermal and Mass Analysis via CFD. *Diffus. Found.* **2020**, *25*, 133–153. [CrossRef]
18. Araújo, M.D.V.; Correia, B.R.D.B.; Brandão, V.A.A.; De Oliveira, I.R.; Santos, R.S.; Neto, G.L.D.O.; Silva, L.P.D.L.; De Lima, A.G.B. Convective Drying of Ceramic Bricks by CFD: Transport Phenomena and Process Parameters Analysis. *Energies* **2020**, *13*, 2073. [CrossRef]
19. Santos, R.S.; Delgado, J.M.P.Q.; Silva, F.A.N.; Azevedo, A.C.; Neto, S.R.F.; Farias, F.P.M.; de Lima, A.G.B.; de Lima, W.M.P.B.; Lima, E.S. Behind the Manufacturing of Industrial Clay Bricks: Drying Stage Predictions Using CFD. *Adv. Mater. Sci. Eng.* **2022**, *2022*, 5530362. [CrossRef]
20. Da Silva, A.V.; Delgado, J.; Guimarães, A.; De Lima, W.B.; Gomez, R.S.; De Farias, R.P.; De Lima, E.S.; De Lima, A.B. Industrial Ceramic Blocks for Buildings: Clay Characterization and Drying Experimental Study. *Energies* **2020**, *13*, 2834. [CrossRef]
21. Lima, E.S.; Delgado, J.M.P.Q.; Guimarães, A.S.; Lima, W.M.P.B.; Santos, I.B.; Gomes, J.P.; Santos, R.S.; Vilela, A.F.; Viana, A.D.; Almeida, G.S.; et al. Drying and Heating Processes in Arbitrarily Shaped Clay Materials Using Lumped Phenomenological Modeling. *Energies* **2021**, *14*, 4294. [CrossRef]
22. Silva, S.K.B.M.; Araújo, C.J.; Lima, A.G.B. Parameters estimation of the drying process of industrial ceramic bricks via concentrated analysis model. *Res. Soc. Dev.* **2021**, *10*, e57210716913. [CrossRef]
23. Brown, A.E. *Brick Drying: A Practical Treatise on the Drying of Bricks and Similar Clay Products*; Franklin Classics: Minneapolis, MN, USA, 2018; p. 236.
24. Gualtieri, A.F.; Ricchi, A.; Gualtieri, M.L.; Maretti, S.; Tamburini, M. Kinetic study of the drying process of clay bricks. *J. Therm. Anal. Calorim.* **2015**, *123*, 153–167. [CrossRef]
25. Dogru, A.K.; Camcioglu, E.; Ozgener, O.; Ozgener, L. Thermodynamics analysis of biomass fired brick drying process. *Int. J. Exergy* **2021**, *35*, 421. [CrossRef]
26. Ndukwu, M.C.; Bennamoun, L.; Simo-Tagne, M.; Ibeh, M.I.; Abada, U.C.; Ekop, I.E. Influence of drying applications on wood, brick and concrete used as building materials: A review. *J. Build. Pathol. Rehabil.* **2021**, *6*, 24. [CrossRef]

27. Karagiannis, N.; Karoglou, M.; Bakolas, A.; Krokida, M.; Moropoulou, A. Drying kinetics of building materials capillary moisture. *Constr. Build. Mater.* **2017**, *137*, 441–449. [CrossRef]
28. Pujari, A.S.; Bhosale, C.H.; Wagh, M.M.; Shinde, N.N. Effect of Temperature on Drying Rate of Various Types of Bricks. *Int. Res. J. Eng. Technol. IRJET* **2016**, *3*, 2793.
29. Silva, S.K.B.M.; Araújo, C.J.; Lima, A.G.B. Numerical analysis of the dimensional variation in structural ceramic blocks during the drying process. *Res. Soc. Dev.* **2021**, *10*, e33310615680. [CrossRef]
30. Robalo, T.C.G. Generalized Hypergeometric Series in the Context of the Theory of Hypercomplex Functions. Master´s Thesis, Mathematic, University of Aveiro, Aveiro, Portugal, 2006. Available online: https://ria.ua.pt/handle/10773/2878?locale=pt_PT (accessed on 6 June 2022).
31. Seaborn, J.B. *Hypergeometric Functions and Their Applications*; Springer Science & Business Media: New York, NY, USA, 2013. [CrossRef]
32. Figliola, R.S.; Beasley, D.E. *Theory and Design for Mechanical Measurements*; John Wiley and Sons: New York, NY, USA, 1995.